Biosensors and Bioelectronics 191 (2021) 113468

Contents lists available at ScienceDirect

Biosensors and Bioelectronics

journal homepage: www.elsevier.com/locate/bios

# Gold nanoparticle-assisted SELEX as a visual monitoring platform for the development of small molecule-binding DNA aptasensors

Eun-Song Lee [a,b], Eun-Ji Kim [a,1], Tae-Ki Park [a], Da-Woon Bae [c], Sun-Shin Cha [c], Tae-Wuk Kim [a,b,d,**], Young-Pil Kim [a,b,d,e,*]

[a] Department of Life Science, Hanyang University, Seoul, 04763, Republic of Korea
[b] Research Institute for Convergence of Basic Sciences, Hanyang University, Seoul, 04763, Republic of Korea
[c] Department of Chemistry and Nanoscience, Ewha Womans University, Seoul, 03760, Republic of Korea
[d] Research Institute for Natural Sciences, Hanyang University, Seoul, 04763, Republic of Korea
[e] Department of HY-KIST Bio-Convergence, Hanyang University, Seoul, 04763, Republic of Korea

ARTICLE INFO

*Keywords:*
Aptamers
Gold nanoparticle
SELEX
Biosensor
Colorimetry
Brassinolide
Bisphenol

ABSTRACT

To resolve time-consuming and imperceptible monitoring problems in the traditional systematic evolution of ligands by exponential enrichment (SELEX), we report gold nanoparticle-assisted SELEX (GNP-SELEX) as a visual, proofreading, and self-monitoring platform and its application to small molecule-binding single-stranded DNA (ssDNA) aptasensors. Through the colorimetric changes between rounds, GNP-SELEX enabled the rapid determination of target-specific aptamer library enrichment with neither target modification nor extra monitoring process. We identified ssDNA aptamers with high selectivity and binding affinity by targeting two small molecules (brassinolide; BL and bisphenol A; BPA) as a model. The rational design of selected aptamers by 3D molecular simulation increased their ability to detect BL or BPA in real samples as bioreceptors. These results suggest that GNP-SELEX is useful as a self-monitoring platform to discover ssDNA aptamers as well as to develop aptasensors for diverse targets in a rapid and simple way.

## 1. Introduction

Single-stranded DNA (ssDNA) aptamers have garnered increasing attention as artificial bioreceptors, given their high chemical stability and cost-effective production, which enables unique studies in biosensing applications (Cho et al., 2009; Gold et al., 1995). While ssDNA aptamers have been determined to detect metal ions, small molecules, proteins, and cells, traditional approaches for the selection of target-specific aptamers involve a process known as systematic evolution of ligands by exponential enrichment (SELEX) and require chemical modifications of target molecules and a supporting matrix (e.g., chip substrate, bead, carrier, or membrane) that binds to a target (Li et al., 2009; Ma et al., 2015; Ruscito and DeRosa, 2016; Strehlitz et al., 2008). Despite the recent advances in modification- or matrix-free methods coupled with capillary electrophoresis, graphene oxide, or click chemistry, the SELEX procedure is still challenging given that a pool of positively or negatively enriched aptamer libraries cannot be directly monitored in sequential rounds (Mendonsa and Bowser, 2004; Nguyen et al., 2014; Pfeiffer et al., 2018). To this end, there is a need for the auxiliary use of high-performance liquid chromatography, enzyme-linked oligonucleotide assay, or real-time quantitative polymerase chain reaction (qPCR) as a monitoring tool to determine intervention and enrichment of the selection pressure of aptamer library in the SELEX process (Drolet et al., 1996; Luo et al., 2017; Muller et al., 2008). In particular, when targeting small molecules, it is challenging to estimate the binding affinity and specificity of the aptamer library for the target molecule in and between rounds (Ruscito and DeRosa, 2016). Surface plasmon resonance, isothermal titration calorimetry, or fluorescence polarization/anisotropy have been generally used to elucidate the binding affinity of the selected aptamers for a small molecule (Chang et al., 2014; Yang et al., 2019; Zhu et al., 2012). However, their repeated use per SELEX round is limited in terms of time and cost. An efficient self-monitoring method during SELEX procedure, enables the rapid enrichment of target-specific aptamers by reducing false-positive and

* Corresponding author. Department of Life Science, Hanyang University, Seoul, 04763, Republic of Korea.
** Corresponding author. Department of Life Science, Hanyang University, Seoul, 04763, Republic of Korea.
*E-mail addresses:* twgibio@hanyang.ac.kr (T.-W. Kim), ypilkim@hanyang.ac.kr (Y.-P. Kim).
[1] Current address: VIB-UGENT Center for Plant Systems Biology, Technologiepark 71, 9052 Zwijnaarde, Belgium.

https://doi.org/10.1016/j.bios.2021.113468
Received 17 February 2021; Received in revised form 9 June 2021; Accepted 26 June 2021
Available online 30 June 2021
0956-5663/© 2021 Elsevier B.V. All rights reserved.

false-negative aptamer libraries.

As a rapid and straightforward analysis, gold nanoparticle (GNP)-based colorimetry, which is caused by size-dependent light scattering and surface plasmon effects, has been widely used with ssDNA aptamers for the visual detection of targets (Huang et al., 2005; Liu and Lu, 2005; Smith et al., 2016). It is noteworthy that target-bound and target-unbound ssDNA aptamers on the surface of GNPs are readily discerned through their aggregation and color change at high salt concentrations (Gopinath et al., 2014; Lee et al., 2018; Wei et al., 2007). This colorimetric principle by aptamer-facilitated GNPs, however, has only been used as a bioassay with a target-specific aptamer sequence. Although GNP-combined SELEX has been recently reported (Chatterjee et al., 2020; Li et al., 2019; Smith, 2014), GNPs were exploited only as a binding matrix of the DNA library, not as a colorimetric tracer or a proofreading platform. Because GNPs can react differently to aptamer libraries in increasing SELEX rounds, this principle prompts us to explore the possibility of colorimetric SELEX.

Here, we report a GNP-assisted SELEX (GNP-SELEX) method as a visual monitoring platform for the rapid development of small molecule-binding ssDNA aptasensors. GNPs in the SELEX process can function as both a colorimetric indicator and an aptamer library selector. The color change in GNPs expressed as extinction ratio ($E_{520}/E_{700}$) enables easy monitoring of an increase or decrease in the binding affinity of the aptamer library against a target molecule (or a counter-target molecule) per round, which does not encompass target modification or post-SELEX analysis (e.g., qPCR). Through dispersion (reddish color) or salt-induced aggregation (purple color) of GNPs during alternating positive and negative SELEX rounds, this method enables the visual evolution of target-selective ssDNA library enrichment and the rapid determination of transition (or termination) of successive rounds. To demonstrate the usefulness of our method, a plant steroid hormone (brassinolide; BL) and an endocrine disruptor (bisphenol A; BPA) were employed as target small molecules with different chemical structures. By optimizing the SELEX conditions, we discovered and engineered ssDNA aptamers against two small molecules, thereby exploring the usability of aptasensors using the selected aptamers.

## 2. Material and methods

### 2.1. Material

Hydrogen tetrachloroaurate (III) trihydrate ($HAuCl_4{\cdot}3H_2O$), sodium citrate dihydrate (trisodium salt, $C_6H_5Na_3O_7{\cdot}2H_2O$), hydrogen peroxide ($H_2O_2$, 30% (w/w)), bisphenol A (2,2-bis(4-hydroxyphenyl)propane, BPA), bisphenol S (bis(4-hydroxyphenyl) sulfone, BPS), and bisphenol F (bis(4-hydroxyphenyl)methane, BPF) were purchased from Sigma-Aldrich (St. Louis, MO, USA). Plant steroids were kindly provided by Dr. Seong-Ki Kim (Chung-Ang University, Seoul, Korea), and 3,3′,5,5′-Tetramethylbenzidine (TMB) was purchased from Thermo Fisher Scientific (Waltham, MA, USA). The Taq polymerase and T-vector were purchased from Promega Corporation (Madison, WI, USA). Agarose gel cleanup kit was purchased from QIAGEN (Hilden, Germany). Ordinary and BPA-free thermal paper receipts were purchased from Hansol Paper Co., Ltd. (Seoul, Korea). Transparent 96-well microplates were purchased from SPL Life Sciences Co., Ltd. (Pocheon, Korea). The combinatorial ssDNA library was synthesized by Integrated DNA Technologies Inc. (IDT, Coralville, IA, USA). Aptamers and primers were synthesized by Macrogen Inc. (Seoul, Korea). A biotinylated aptamer was synthesized by Macrogen Inc. (Seoul, Korea).

### 2.2. Synthesis of GNP

Unmodified GNPs were synthesized by reduction and stabilization with sodium citrate as previously described (Grabar et al., 1995; Turkevich et al., 1951). Briefly, 100 μL of a stock solution containing 300 mM $HAuCl_4{\cdot}3H_2O$ was added to 50 mL distilled water to yield a final concentration of 600 μM in a round-bottomed flask. This solution was then boiled under vigorous stirring. One milliliter of a 2% (w/v) sodium citrate solution was added to the stirring solution. This resulted in a color change from pale yellow to reddish-brown. The solution was then boiled for another 20 min and then cooled to room temperature while stirring. The gold colloid was stored at 4 °C until further use. The sizes of dispersed or aggregated GNPs were characterized using a dynamic light scattering instrument (Scatteroscope I; K-ONE Inc., Seoul, Korea). The molar concentration of the unmodified GNPs solution was determined to be 1.0 nM after confirming the size distribution and particle number of the colloidal GNP. The extinction coefficient of the unmodified GNPs was $1.26 \times 10^9\ M^{-1}\ cm^{-1}$ at 520 nm.

### 2.3. Preparation of the ssDNA library

Prior to SELEX, a 60-nt ssDNA library, including a central 30-nt randomized sequence flanked by two 15-nt primer binding sites, was prepared using a forward primer (5′−ATGCGGATCCCGCGC−3′) and reverse primer (5′−CGCGCGAAGCTTGCG−3′). After incubation with primers in the ratio of 10:1 (forward: reverse), the ssDNA library was amplified by asymmetric PCR with one cycle at 95 °C for 5 min and 30 cycles at 95 °C for 30 s, 57 °C for 30 s, and 72 °C for 30 s, followed by the last cycle at 72 °C for 10 min. The PCR products were analyzed using 3% agarose gel electrophoresis (100 V, 30 min) in 0.5 × Tris-acetate-EDTA (TAE) buffer and purified using a gel extraction column. The product was eluted with a 0.3 M sodium acetate solution (pH 5.2) and concentrated using ethanol precipitation. 30 pmol of the random ssDNA library (final 150 nM) was incubated with 0.075 pmol GNPs (final 0.375 nM) at a molar ratio of 400:1 (ssDNA:GNP) in a binding buffer (0.1 × phosphate-buffered saline (PBS), pH 7.4, containing 1 mM $PO_4^{3-}$, 13.7 mM NaCl, and 0.27 mM KCl) to give a final volume of 200 μL, followed by centrifugation at 6,500×*g* for 10 min to eliminate the ssDNA library with low affinity for the GNP surface prior to SELEX. The supernatant was then discarded, and the pulldown product was washed three times with the binding buffer. After the product was boiled at 95 °C for 15 min and centrifuged again, the eluted ssDNA library was collected in the binding buffer for use in the first round of SELEX.

### 2.4. GNP-SELEX procedure

A SELEX process was performed to select ssDNA aptamers binding specifically to BL or BPA, containing successive steps of negative and positive selections using GNPs and target or counter-target small molecules (Tables S1 and S2). During the first step of each round, the ssDNA library was initially mixed with GNPs in a binding buffer at a molar ratio of 400:1 (ssDNA library:GNP) to render a final volume of 190 μL in a transparent 96-well microplate (SPL Life Sciences). In the second step, 10 μL of a solution containing a target molecule (for the positive SELEX) or a counter-target molecule (for the negative SELEX) was added to the library-GNP colloidal solution and incubated for 30 min. During the third step, 10 μL of 1 M NaCl was added to the solution and incubated for 15 min to induce salt-bridged aggregation. In the fourth step, the supernatant GNP-unbound ssDNA library (for the positive SELEX) or GNP-bound ssDNA library (for the negative SELEX) was collected by centrifugation (at 6,500×*g* for 10 min), followed by concentration using ethanol precipitation; GNP-bound ssDNA library was additionally subjected to boiling at 95 °C for 15 min and subsequent centrifugation prior to concentration. In the last step, to amplify double-stranded (dsDNA) from the eluted ssDNA library, 2 μL of ssDNA library from SELEX was mixed with 25 μL of 2 × Hot Start GoTaq master mix (Promega, Madison, WI, USA), 21 μL of distilled water, 1 μL of 25 μM forward primer, and 1 μL of 25 μM reverse primer and subjected to 30 cycles of regular PCR. The PCR product was monitored using 3% agarose gel electrophoresis (100 V, 30 min) and purified by agarose gel extraction. To generate the ssDNA library for the next round, asymmetric PCR was performed with dsDNA. To monitor steps 1–3 in each SELEX round, the

extinction values of the solutions were sequentially measured using a microplate reader (Varioskan; Thermo Fisher Scientific), and the color photographic image of each solution was sequentially captured using a mobile phone camera (Galaxy Note 8, Samsung Electronics, Suwon, Korea). The aggregation of colloidal GNP was estimated from the extinction ratio ($E_{520}/E_{700}$), where $E_{520}$ and $E_{700}$ represent the extinction value of the colloidal GNP at 520 nm and 700 nm, respectively.

### 2.5. Sequencing

In the last round of SELEX, dsDNA amplified from the selected aptamers was subcloned into a pGEM-T Easy plasmid vector (Promega) to retrieve the entire sequence. The plasmid was transformed into *E. coli* DH5α, followed by an incubation step at 37 °C under selective antibiotic pressure. Individual bacterial colonies were sequenced, and the multiple alignments of selected aptamers were performed using ClustalX to analyze the group similarity. The secondary structure of the aptamer candidates was predicted using Mfold web server (Zuker, 2003). Consensus motif of aptamer candidates was determined using Multiple Em for Motif Elicitation (MEME, http://meme-suite.org/tools/meme/) (Bailey et al., 2009).

### 2.6. Determination of binding affinity of aptamers for small molecules using the GNP colorimetric assay

To determine the binding affinity of selected aptamers for small molecules, an ssDNA aptamer (30 μL of 10 μM) was initially mixed with GNPs (75 μL of 1 nM) in a binding buffer to render a final volume of 190 μL in a transparent 96-well microplate. The solution was then reacted with 10 μL of various concentrations of small molecules in the binding buffer, which was incubated for 30 min at room temperature. After incubation, 10 μL of 1 M NaCl was added to the solution. The extinction ratio ($E_{520}/E_{700}$) of the solutions was measured using a microplate reader and the color photographic image of each solution was captured using a mobile phone camera. The dissociation constant ($K_D$) value was calculated by employing binding (%) as a function of target concentration using the GNP colorimetric assay. The value represents a target concentration at which half of the maximal binding (%) reached in the hyperbolic curve fitted by a single-site model. Binding (%) indicates the proportion of target-dependent extinction ratio changes relative to that of the target-independent extinction ratio change, according to the following Equation (1):

$$\text{Binding}\ (\%) = \frac{\text{Ext}_{R0} - \text{Ext}_{RC}}{\text{Ext}_{R0} - \text{Ext}_{Rmax}} \times 100 \quad \text{(Eq.1)}$$

where $\text{Ext}_{R0}$ is the salt-induced extinction ratio ($E_{520}/E_{700}$; $\text{Ext}_R$) in the absence of the target, $\text{Ext}_{RC}$ is the salt-induced $\text{Ext}_R$ in the presence of a specific target concentration, and $\text{Ext}_{Rmax}$ is the salt-induced maximal $\text{Ext}_R$ without an aptamer.

### 2.7. Circular dichroism (CD)

CD spectra from the ssDNA aptamer were analyzed using a Jasco J-1500 CD spectrophotometer (Jasco, Japan) equipped with a thermal controlled single cell block. Aptamers (final 0.7–1 μM) with or without the target molecule (final 1–10 μM) were scanned between 200 nm and 350 nm at a speed of 100 nm $\text{min}^{-1}$ in a 1 nm bandwidth. The CD curves were averaged from three scans. Data were corrected against a blank measurement of binding buffer and smoothed using a Savitzky–Golay filter.

### 2.8. Preparation of plant extracts

Wild-type *Arabidopsis thaliana*, Col-0, and brassinosteroid-deficient mutant *Sdet2* seeds were sterilized with 70% ethanol containing 0.025% Triton X-100 and planted on 1/2 Murashige and Skoog (MS; Duchefa Biochemie, Haarlem, Netherlands) medium containing 0.8% Phytoagar and 1% sucrose (Park et al., 2014). After two days of cold treatment, plants were grown under long-day conditions (16 h/8 h light-dark cycle) in a plant growth chamber at 22 °C. For BL treatment, seedlings were grown on 1/2 MS medium with or without 100 nM BL. The 10-day-old *Arabidopsis* seedlings (0.6 g) were ground using a mortar and pestle and extracted with 8 mL of 80% methanol in water three times. The extracts were concentrated in vacuo. The dried fraction was dissolved in a small amount of 100% methanol prior to use.

### 2.9. Detection of BL in plant extracts by aptamer-mediated precipitation (AP)

Prior to AP, agarose beads were conjugated with an anti-BL ssDNA aptamer (tgBL-v2) via streptavidin-biotin interaction. Twenty microliters of streptavidin-coated agarose resin (Life Technologies, CA, USA) were washed twice with 1 × bind and wash (B&W) buffer (5 mM Tris-HCl, pH 7.5, containing 0.5 mM EDTA and 1 M NaCl) and resuspended in 500 μL of 2 × B&W buffer to inhibit ssDNA degradation during the aptamer binding to the agarose bead. The 5′-end biotinylated tgBL-v2 aptamer in distilled water was mixed with agarose resin to render a final concentration of 3.6 μM, followed by a 15 min incubation at room temperature on a shaker. The mixture was washed twice with a 1 × B&W buffer to remove the excess aptamers. The aptamer-conjugated beads were kept in 20 mM Tris-HCl (pH 7.4) at 4 °C. For the AP procedure, 30 μL of plant extract was diluted in 70 μL of 100% ethanol and centrifuged at 13,000×*g* for 3 min to remove hydrophobic debris. 50 μL of supernatant was diluted in an AP buffer (20 mM Tris-HCl, pH 7.4, containing 0.1 mg $\text{mL}^{-1}$ salmon sperm DNA) and then mixed with the aptamer-conjugated bead. In this step, divalent ions were omitted in buffer because high salt concentrations increase non-specific interactions between the aptamers and other hormones. After 10 min-incubation, the bead was sequentially washed with PBST (PBS containing 0.05% Tween-20) and the AP buffer. To elute BL from the beads, 100% ethanol was mixed with the beads and the eluate was collected by centrifugation (13,000×*g* for 5 min).

### 2.10. Detection of BPA on thermal receipts by an enzymatic aptasensor

Prior to the assay, the tgBPA-v2 aptamer was boiled for 5 min at 95 °C, and slowly cooled at room temperature for 15 min. The tgBPA-v2 aptamer (10 μL of 10 μM), hemin (10 μL of 10 μM), and BPA (5 μL at appropriate concentration) were mixed with 25 μL of 2 × PBS. The final concentrations of aptamer and hemin were 2 μM. For the process of binding, the mixture was incubated for 10 min at room temperature. TMB solution (100 μL) containing TMB and 0.1% hydrogen peroxide was then added to the mixture. When the color of the solution changed from clear to blue (~5 min), the absorbance was measured using a microplate reader. For the detection of BPA on thermal receipt papers, the receipt paper, cut into a square size (0.75 × 0.75 cm), was passivated with 500 μL of binding buffer containing 0.2 mg $\text{mL}^{-1}$ salmon sperm DNA (SSD) in a transparent 12-well microplate (SPL Life Sciences) at room temperature, for 30 min. Excess SSD was washed away with 500 μL of binding buffer for 3 min. Then, 500 μL of reaction solution containing 400 nM tgBPA-v2 and 400 nM hemin in the binding buffer was dropped on the paper, followed by a 10 min incubation at room temperature. The TMB solution containing 0.1% hydrogen peroxide was sequentially dropped on the paper to induce a color change. After 5 min of incubation, the color photographic image of the paper was taken using a mobile phone camera (Galaxy Note 8), and the TMB intensity was calculated by ImageJ software (University of Wisconsin at Madison, Madison, WI, USA).

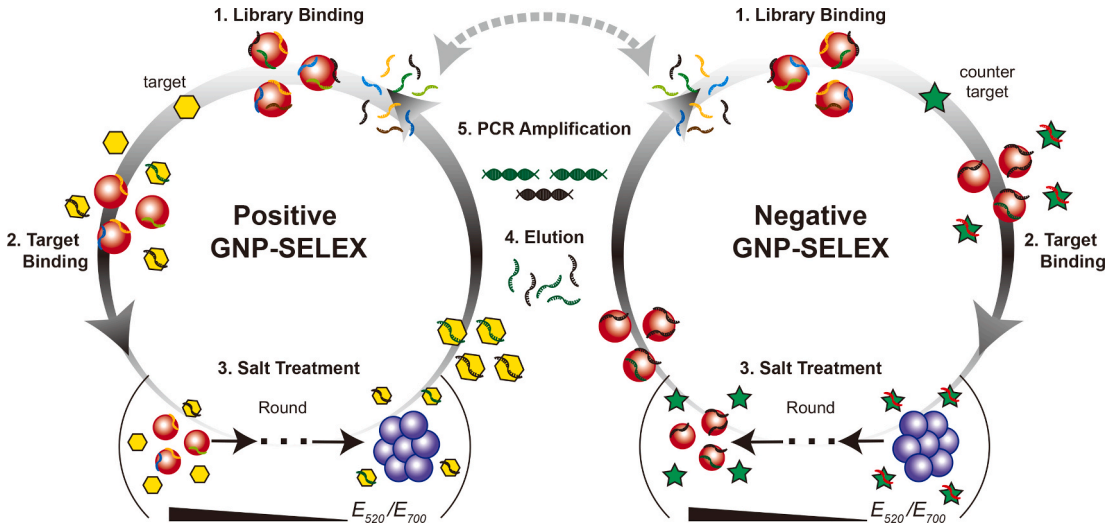


**Scheme 1.** Schematic of the GNP-SELEX procedure. Positive and negative GNP-SELEX are alternately used for the target molecules (in yellow) and the counter-target molecules (in green), respectively, to discover the target-selective ssDNA aptamers. Owing to the salt-induced dispersion (reddish color) or aggregation (purple color) of GNPs during the iterative rounds, this method simplifies the monitoring of the visual evolution of the target-selective ssDNA library enrichment and the determination of the transition (or termination) of the successive rounds. The positive or negative GNP-SELEX is interchangeable at the beginning of each round (dotted arrow) and consists of five steps each.

### 2.11. Statistical analysis

Statistical analysis was performed using the SPSS software program (IBM, version 26.0). Statistical significance was determined by Student's *t*-test or one-way ANOVA as indicated in the figure legends. All data sets were subjected to normality tests (Shapiro-Wilk test) when applicable. Based on the normality of distributions, Student's t-test or one-way ANOVA with Scheffe's post-hoc test was performed only if the data set are truly normal. *N*-values correspond to the sample size and *p*-values are ranged as follows: $*p < 0.05$; $**p < 0.01$; $***p < 0.001$.

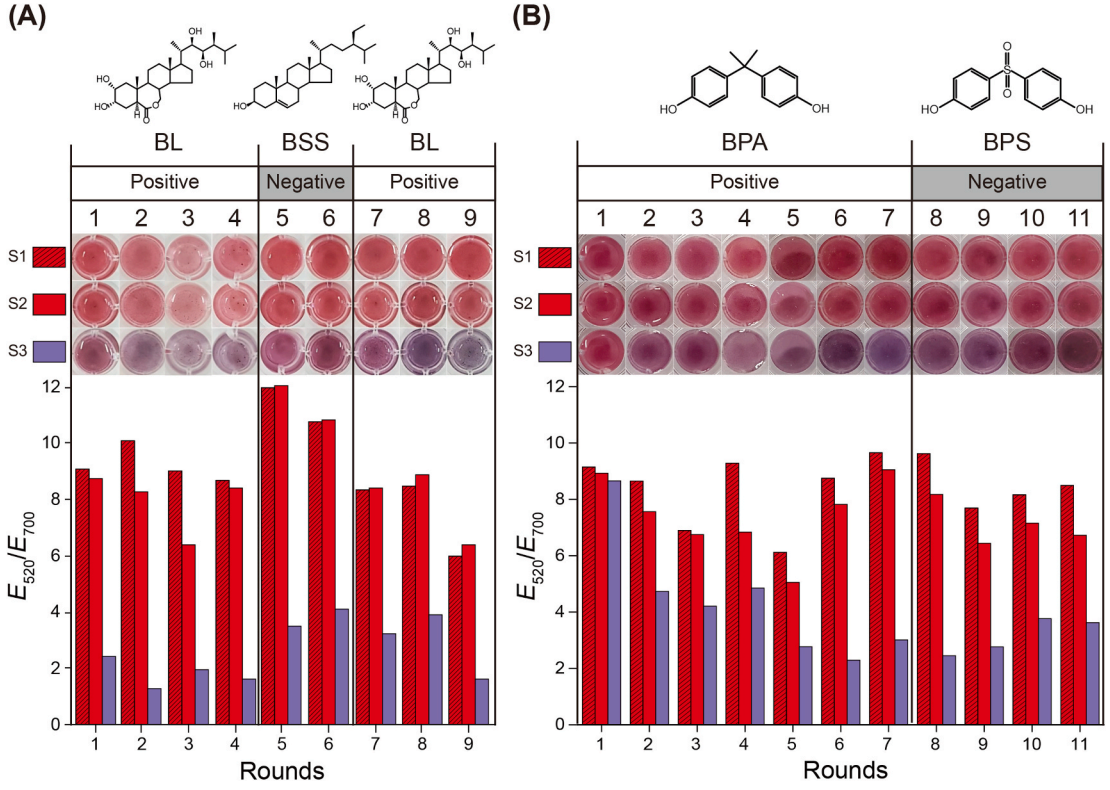


**Fig. 1.** GNP-SELEX for the discovery of ssDNA aptamers against BL (A) or BPA (B). Color change (image in microplate well) and extinction ratio value ($E_{520}/E_{700}$; bar graph) of the colloidal GNP observed with the progression of each SELEX round are displayed here. Positive GNP-SELEX was performed with target molecules (BL or BPA), whereas negative GNP-SELEX with counter-target molecules (BSS or BPS). S1, S2, and S3 represent step 1 (aptamer library binding), step 2 (target or counter-target binding), and step 3 (salt treatment) of the colloidal GNP in each round, respectively. (For interpretation of the references to color in this figure legend, the reader is referred to the Web version of this article.)

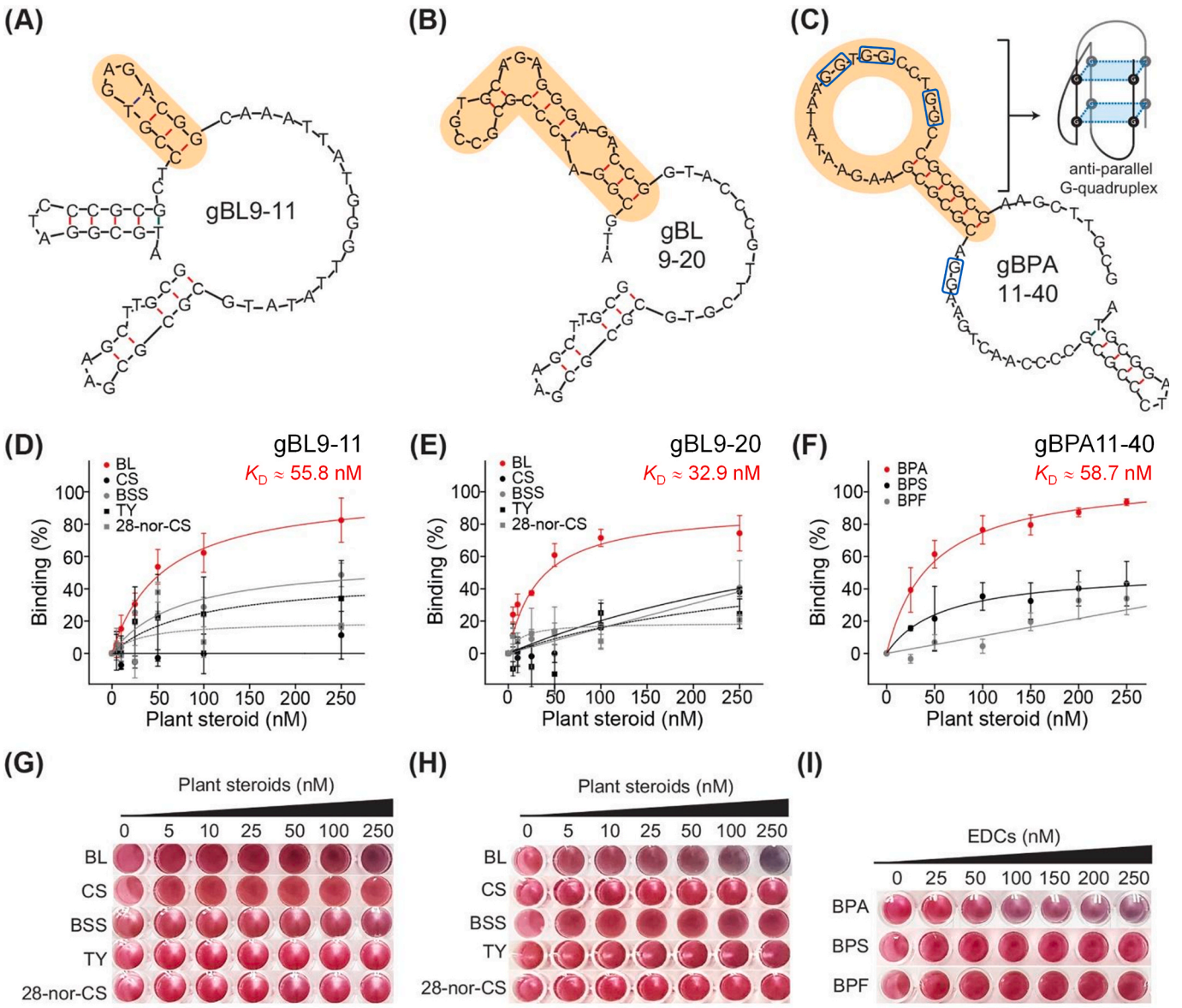


**Fig. 2.** Binding affinity test of candidate aptamers. (A–C) Secondary structures of the candidate aptamers (gBL9-11, gBL9-20, and gBPA11-40). Major hairpin structures for target binding have been indicated in orange and G4 in blue. (D–F) GNP-based binding affinities of candidate aptamers. Binding (%) indicates the proportion of changes in the target-dependent extinction ratio relative to that of the target-independent extinction ratio (see Experimental procedures in the supporting information). $K_D$ value was calculated from the binding (%) as a function of the target concentration using the GNP colorimetric assay. (G–I) Photographs showing the GNP colorimetric assay. CS, castasterone; TY, typhasterol; 28-nor-CS, 28-norcastasterone; EDC, endocrine disrupting chemical; BPF, bisphenol F. (For interpretation of the references to color in this figure legend, the reader is referred to the Web version of this article.)

## 3. Results and discussion

### *3.1. GNP-SELEX enables the rapid, proofreading, and self-monitored enrichment of ssDNA aptamer library*

As depicted in Scheme 1, the positive GNP-SELEX undergoes five steps repeatedly: binding of the ssDNA library to the GNPs, target binding, salt treatment, elution, and PCR amplification. The ssDNA library (60-nt in length containing a 30-nt random region) stabilizes the unmodified GNPs (citrate-capped GNPs) using the van der Waals forces between the hydrophobic nitrogen bases and the GNP surface (ssDNA library binding step). The addition of the target molecules to the ssDNA-stabilized GNPs induces a conformational change in some ssDNA sequences. This results from the increase in the affinity of the target-nitrogen base to a level higher than that of the Au-nitrogen base affinity, leading to the release of the ssDNA from the GNPs (target binding step). This brings about the rapid aggregation of the GNPs (lower $E_{520}/E_{700}$ value) under high-salt conditions, resulting in the color changes in the colloidal GNP from reddish to purple, with the progression of each iterative round (salt treatment step). The ssDNA library released from the GNPs can then be easily harvested from the supernatant after centrifugation, followed by PCR amplification (elution and PCR amplification steps). To endow the ssDNA library target specificity, negative GNP-SELEX can be performed with the counter-target molecules. The opposite color change (higher $E_{520}/E_{700}$ value), relative to the positive GNP-SELEX, enables easy monitoring to remove the unspecific ssDNA strands.

Two small molecules, BL and BPA, were chosen as targets to demonstrate the possibility of GNP-SELEX. BL is the most biologically active brassinosteroid (BR). BRs are steroid hormones essential for plant growth and development (Noguchi et al., 2000; Thompson et al., 1981). The endogenous BL level in vegetative tissue is extremely low;

**Table 1**
List of oligonucleotide sequences used in the study.

| Oligo Name | Sequence (5′–3′) | Length (nt) |
|---|---|---|
| Aptamer library[a] | ATG CGG ATC CCG CGC–$N_{30}$–CGC GCG AAG CTT GCG | 60 |
| Forward primer | ATG CGG ATC CCG CGC | 15 |
| Reverse primer | CGC AAG CTT CGC GCG | 15 |
| gBL9-11 | ATG CGG ATC CCG CGC TCC GTG AGA CGG CAA ATT ATG GGT TAT ATG CGC GCG AAG CTT GCG | 60 |
| gBL9-20 | ATG CGG ATC CCG CGC CGT GCA GAG GGA GAC CGG TAC CCG TTC GTG CGC GCG AAG CTT GCG | 60 |
| gBPA11-40[b] | ATG CGG ATC CCG CGC CCC AAC TGA AGG ACG CGC GAA GAA TAT AAG GTG GCC TGG CGC GCG AAG CTT GCG | 70 |
| tgBL-v1 | CGG ATC CCG CGC CGT GCA GAG GGA GAC CG | 29 |
| tgBL-v2[c] | GCG GAT CCC GCG CCG TGC AGA GGG AGA CCG **C** | 31 |
| tgBPA-v1 | CGC GCG AAG AAT ATA AGG TGG CCT GGC CGC GCG | 33 |
| tgBPA-v2 | GGA CGC GCG AAG AAT ATA AGG TGG CCT GGC CGC GCG | 36 |
| tgBPA-v3 | GGA CGC GCG AAG AAT ATA AGG TGG CCT GG | 29 |

[a] The primer sequences are underlined.
[b] The short stretch of the aptamer (*i.e.*, insertion of multiple nucleotides into parental sequences) was created during PCR amplification.
[c] This truncated aptamer was mutated in a single sequence marked in a bolic letter.

~0.01–0.1 ng per gram of fresh plant weight (gfw) (Kanwar et al., 2017). Gas chromatography/mass spectrometry-based identification is a traditional method to measure endogenous BL levels in plant tissues. However, it requires a large amount of plant material (tens of grams to tens of kilograms). Additionally, antibodies or aptamers have not been reported for BL, which makes it difficult to detect the amount of BL in the plant tissues. In contrast to BL, BPA, an endocrine disrupting chemical, was reported to identify its ssDNA aptamer, which was directly compared with our selected aptamers (Jo et al., 2011; Xu et al., 2019). When the self-assembly of the GNPs (26.4 nm in core diameter) was controlled by aptamer library at high salt in the absence and presence of the target (Fig. S1), the molar ratio (1:400) of GNP to 30-bp randomized aptamer library was optimized with salt-treated reaction time (15 min) (Fig. S2). An alternating process with positive (with target molecules) and negative GNP-SELEX (with counter-target molecules) was performed to confer with the ssDNA library on the target specificity (Fig. 1). The iterations of positive GNP-SELEX resulted in a decrease in the $E_{520}/E_{700}$ value at high salt concentrations (final 48 mM NaCl) against the BL (Fig. 1A) or BPA (Fig. 1B). In contrast, the negative rounds of GNP-SELEX increased the $E_{520}/E_{700}$ value against the β-sitosterol (BSS) or bisphenol S (BPS) as the target analogs. Interestingly, the salt-induced color change in the colloidal GNP instantly reached saturation with increasing rounds of the BL-targeted GNP-SELEX, but gradually in the BPA-targeted GNP-SELEX, indicating target molecule-dependent SELEX span. This feature can possibly be attributed to the difference in chemical structure, in which BL provided more diversity at the binding sites with aptamer library than BPA. Notably, this method simplifies the determination of whether the next round will proceed with the positive or negative SELEX at the salt-induced step (step 3). For example, the 4th and 6th rounds in Fig. 1A and the 7th SELEX in Fig. 1B enabled the transition from positive to negative SELEX (or vice versa) based on the $E_{520}/E_{700}$ value. Similarly, the rapid recovery of the salt-induced color change in the negative SELEX (in Fig. 1A) implied increased loss in the target-specific aptamer pool, facilitating the demand for positive enrichment of the aptamer library through additional positive SELEX. However, little color change in the negative SELEX (Fig. 1B) represents the retention of the target-specific aptamer pool, indicating that some of the enriched aptamer library may bind to BPS with weak binding affinity, which may not result in full recovery of GNP color. In the round where the color change stagnated, we terminated the negative SELEX without additional positive SELEX to prevent loss of target-specific aptamer library. This result reveals that using color change, GNP-SELEX allows for the proofreading and self-monitoring of the positive and negative pressure of the aptamer library against small molecules.

### 3.2. *Fast colorimetric readout of selected aptamers manifests target specificity and binding affinity*

The amplified SELEX product was cloned into a T-vector for sequencing to identify target-specific aptamers. When the nucleotide sequence of approximately 50 clones for each SELEX was aligned by the primary sequence similarity, four groups for BL and five for BPA were clustered based on their frequency (Fig. S3). Two aptamers were chosen for BL (gBL9-11 and gBL9-20) and one for BPA (gBPA11-40) based on the structural stability (ΔG value) by predicting the secondary structure

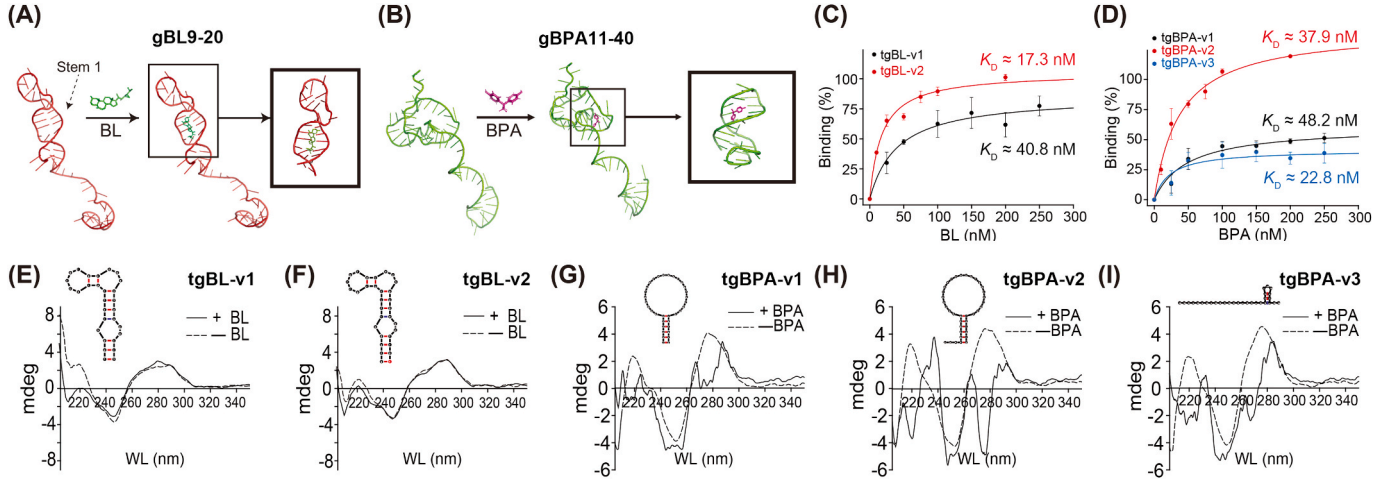


**Fig. 3.** 3D modeling-based engineering of full-length aptamers and binding affinity test of truncated aptamers. (A) 3D molecular simulation of gBL9-20 with BL representing lock-and-key modeling. (B) 3D molecular simulation of gBPA11-40 with BPA representing induced-fit modeling. (C and D) Binding affinity test of the truncated aptamers as a function of target concentration using GNP-based colorimetry. (E and F) CD analysis of tgBL-v1 and tgBL-v2 in the presence (solid line) and absence (dotted line) of BL. (G–I) CD analysis of tgBPA-v1, tgBPA-v2, and tgBPA-v3 in the presence (solid line) and absence (dotted line) of BPA. The final concentrations of aptamers and target small molecule were 1 μM and 2 μM, respectively. Secondary structures of all truncated aptamers have been displayed at the top of the respective CD spectra.

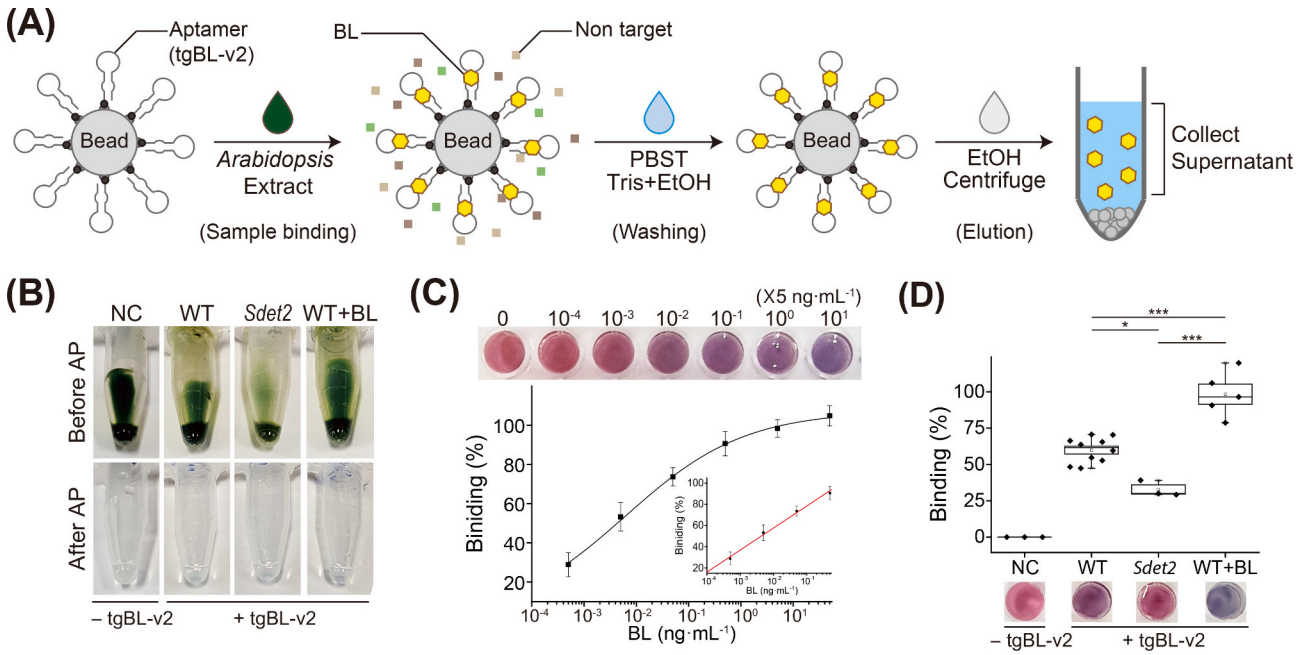


**Fig. 4.** Aptamer-mediated precipitation (AP) and quantitative analysis of BL in crude plant extracts using tgBL-v2. (A) Schematic of purifying BL in plant samples using a tgBL-v2-coated agarose bead. (B) Photographs of *Arabidopsis* extracts before and after AP. NC, negative control with aptamer-free AP in wild-type; WT, *Arabidopsis* wild-type Col-0; *Sdet2*, BL-deficient *Arabidopsis* mutant; WT + BL, WT Col-0 grown on MS medium containing 100 nM BL. (C) Photograph and non-linear regression curve ($R^2 = 0.9977$) of GNP colorimetric assay with tgBL-v2 as a function of BL concentration ($5 \times 10^{-4}$ to $5 \times 10$ ng mL$^{-1}$). The inset graph indicates a linear regression ($R^2 = 0.9899$) over a relatively narrow range ($5 \times 10^{-4}$ to $5 \times 10^{-1}$ ng mL$^{-1}$). Error bars indicate standard error ($n = 4$). (D) Quantitative determination of BL in the extracts from three plant models with NC. The representative color image is shown below the graph. Error bars above and below the box represent maximum and minimum values ($n = 3$–10); significant differences in binding (%) among the tested samples were evaluated (*$p < 0.05$, **$p < 0.01$ and ***$p < 0.001$, one-way ANOVA with Scheffe's post-hoc test). The box plot depicts the data distribution, and the horizontal line that intersects the box is the median value for all the data. The horizontal lines that form the top and bottom of the box are the 75th and 25th percentile, respectively. (For interpretation of the references to color in this figure legend, the reader is referred to the Web version of this article.)

of the aptamer candidates (Fig. 2A and Fig. S4). The sequences of selected aptamers are listed in Table 1. When the consensus motif was determined using MEME from the aptamer sequences, the motifs were components of our selected aptamers, representing a key region of the aptamer for target binding (Fig. S5). Additionally, the gBPA11-40 aptamer has short stretches (i.e., insertion of single or multiple nucleotides into parental sequences) that were accidently created during PCR amplification, similar to the case in the error-prone PCR. This is potentially due to the PCR by-products that can be initiated by the partial binding between primers and random segments of the library sequences, yielding longer DNA products than the parental library sequences, as commonly observed in SELEX (Tolle et al., 2014; Wang et al., 2019). Despite the presence of stretched aptamer pools with adequate sequence diversity, these are considered favorable for increasing the binding affinity of aptamers to the target through the GNP-SELEX. These full-length candidate aptamers exhibited a hammerhead structure containing distinct satellite hairpin regions (highlighted in orange) and G-quadruplex (G4) sequences (marked in blue for gBPA11-40), independent of primer-binding sites (Fig. 2A–2C). When three aptamers were tested to evaluate their ability to specifically bind to targets using GNP-based colorimetric assays, the binding curve observed for each aptamer is shown in Fig. 2D–2I. Fig. S6 represents the chemical structures of the small molecules used. The binding affinities, gBL9-11 ($K_D \approx 55.8$ nM) and gBL9-20 ($K_D \approx 32.9$ nM), were higher in BL than those in other plant steroids. Additionally, the binding affinity of gBPA11-40 ($K_D \approx 58.7$ nM) was higher in BPA than in BPS and BPF. Notably, gBPA11-40 showed higher binding affinity than the reported aptamer (Jo et al., 2011; Lee et al., 2018) under the same conditions (Fig. S7). This result indicates that the aptamers selected through GNP-SELEX have high target specificity, in which the GNPs can simultaneously be used to perform SELEX and determine the target binding affinity.

### 3.3. 3D molecular engineering of full-length aptamers promotes enhanced binding affinity

We further engineered two full-length aptamers (gBL9-20 and gBPA11-40) to achieve stronger binding affinity (Fig. 3). The terminal sequence of each aptamer was truncated without disturbing its target binding site and conformational folding through three-dimensional (3D) modeling and molecular dynamics simulation (Fig. S8). It was predicted that BL could bind to the GC pairs in the major groove (in stem 1) of the gBL9-20 aptamer without a conformational change, similar to the lock-and-key model (Fig. 3A). Contrastingly, BPA was expected to trigger ligand-induced conformational change; the B-form helix in the hairpin structure of the gBPA11-40 aptamer changed into an anti-parallel G4 structure by the BPA (Fig. 3B). Similarly, two truncated aptamers were generated from the gBL9-20, containing essential stem-loop structures without (tgBL-v1) or with an additional GC pair (tgBL-v2). Three truncated aptamers (tgBPA-v1, single hairpin without G4; tgBPA-v2, single hairpin with G4; tgBPA-v3, no hairpin with G4) were also generated from gBPA11-40. When the truncated aptamers were tested with targets using GNP-based colorimetry, binding affinities of the truncated aptamers, tgBL-v2 and tgBPA-v2 ($K_D \approx 17.3$ nM for BL and $K_D \approx 37.9$ nM for BPA, respectively, in Fig. 3C and D), and their target specificity (Fig. S9) was improved compared to those of their full-length aptamers. When isothermal titration calorimetry (ITC) was employed to determine binding thermodynamics of aptamers to small molecules, the binding affinities from heat changes were slightly different from those by GNP-based assay, which may be attributed to different reaction regime and/or equilibrium condition applied when using two assays (Fig. S10). Circular dichroism (CD) analysis further supported the molecular

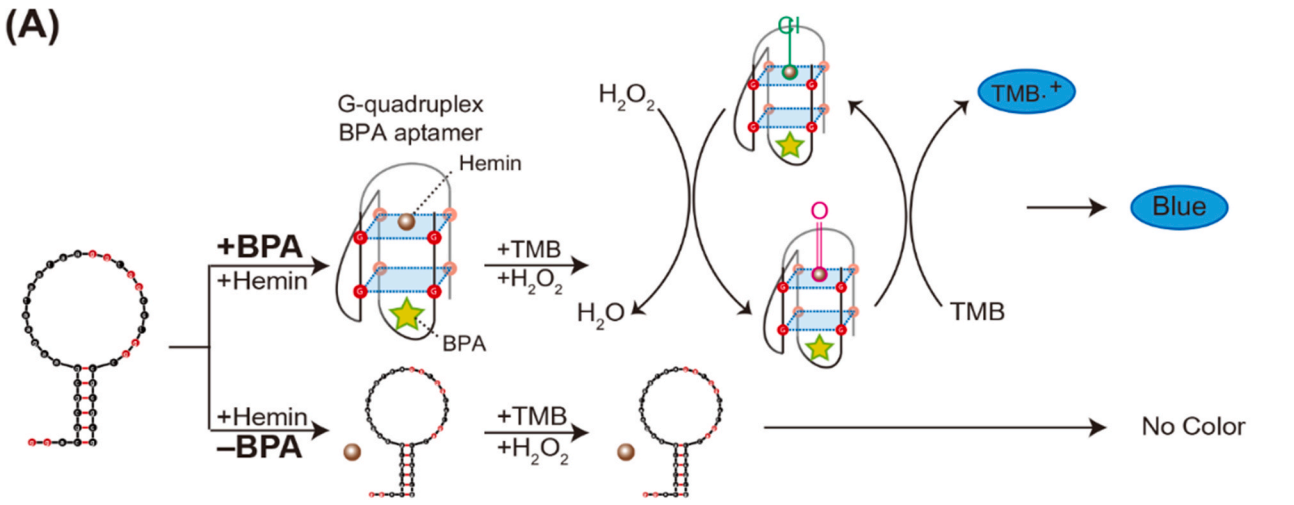


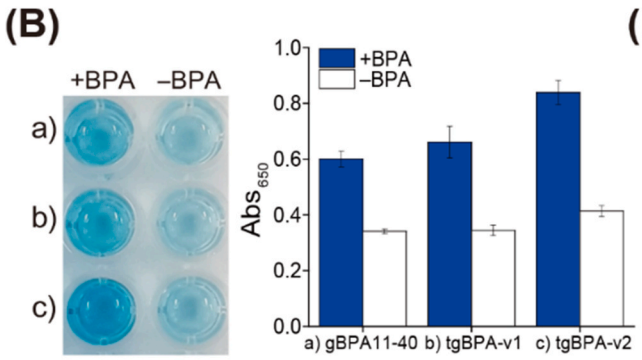


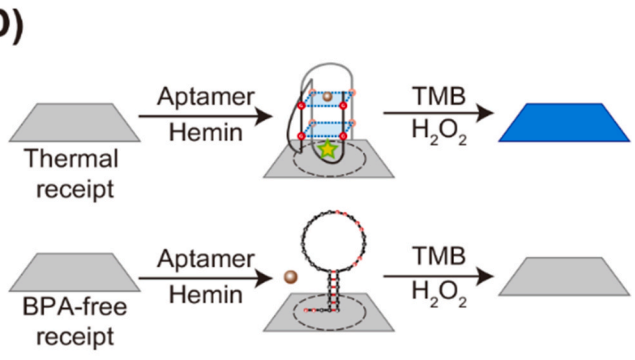


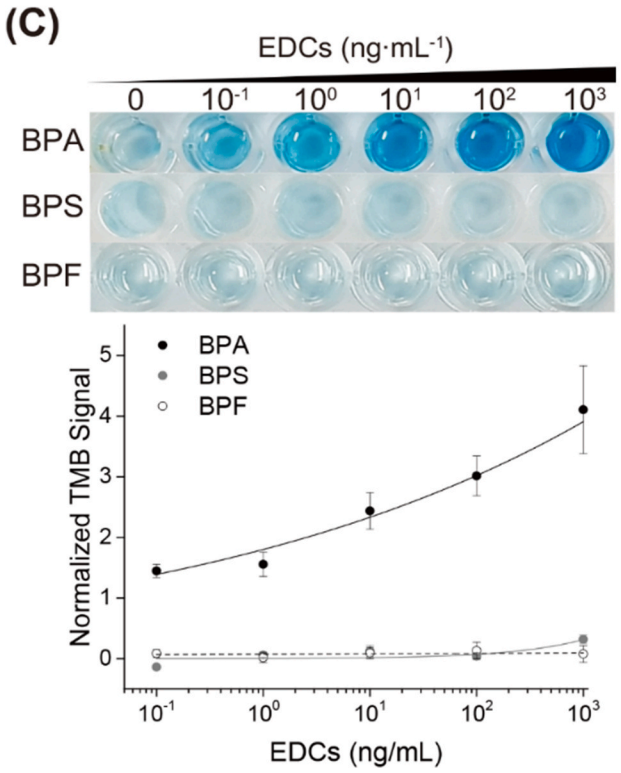


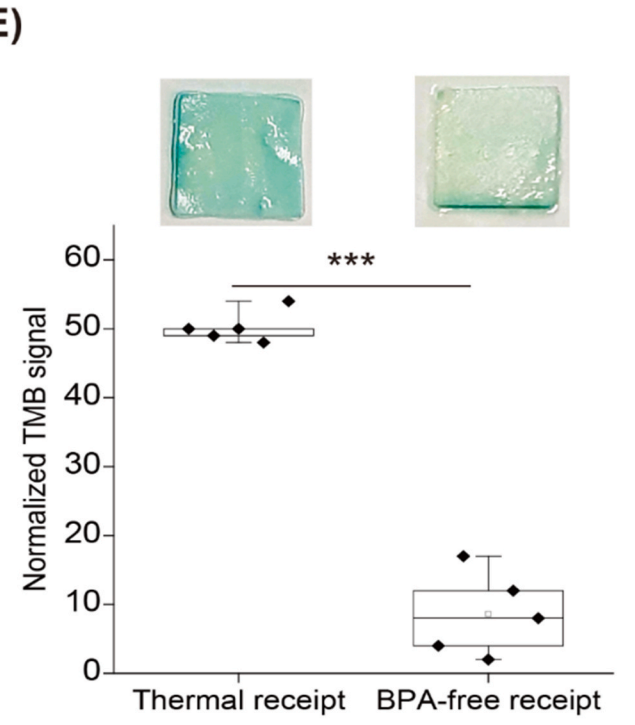


*(caption on next page)*

**Fig. 5.** Aptamer-based enzymatic sensing of BPA on thermal receipts. (A) Schematic of colorimetric detection of BPA based on peroxidase activity of G4-induced aptamers in the presence of hemin and chromogenic reagents (TMB/$H_2O_2$). (B) Photograph (left) and bar graph (right) showing peroxidase activity of three selected aptamers in the presence and absence of BPA in a microwell plate. TMB color intensity was measured at 650 nm absorbance. (C) Photographs (top) and calibration curves (bottom) representing an aptamer/hemin-based color change as a function of BPA, BPS, or BPF concentration ($0-10^3$) in a microwell plate. (D) Schematic of the two-step process for direct detection of BPA by sequentially dropping hemin-bound tgBPA-v2 and TMB/$H_2O_2$ on thermal receipt paper. (E) Photograph (top) and response graph (bottom) of the drop-on assay using tgBPA-v2 on normal and BPA-free thermal receipts. TMB signal was normalized to the background color intensity. Error bars above and below the box represent maximum and minimum values ($n = 5$); significant difference in TMB signals between two receipts was evaluated (***$p < 0.001$, Student *t*-test with Shapiro-Wilk normality test). (For interpretation of the references to color in this figure legend, the reader is referred to the Web version of this article.)

simulation and binding affinity results. There was a considerable change in the hairpin structure at 220 nm in the tgBL-v1 aptamer after binding with BL, rather than with tgBL-v2, reflecting the ligand-independent structure of tgBL-v2 (Fig. 3E and F). The terminal GC pair in tgBL-v2 resulted in minor groove instability compared to tgBL-v1, confirmed by the fluorescence intensity of Hoechst 33258 specific to nucleic acid minor grooves (Zhu et al., 2011) (Fig. S11). Unlike tgBL-v2, tgBPA-v2 showed the most significant change at 270–290 nm in the CD spectrum after binding with BPA, indicating the formation of ligand-induced anti-parallel G4 structure (Fig. 3G, H, and 3I). This conformational change of tgBPA-v2 aptamer increased significantly as the BPA concentration increased (Fig. S12).

### 3.4. ssDNA aptamers via GNP-SELEX potentiate the development of practical bioassay and biosensor

To address the potential of engineered aptamers as biosensing receptors, we designed assay platforms to rapidly detect BL or BPA in real samples (Figs. 4 and 5). Similar to conventional immunoprecipitation used for target purification, tgBL-v2 aptamer-mediated precipitation (AP) was developed to purify BL and remove interferents in the crude extract of *Arabidopsis* (Fig. 4A). Consequently, the pre-treated post-AP reactants (Fig. 4B) were subjected to a GNP-based colorimetric assay to quantitatively determine the amount of BL in the plant extracts from the calibration curve (Fig. 4C). Compared to the negative control (NC) without the aptamer in *Arabidopsis* wild-type Col-0 (WT), a significant difference in BL-induced GNP color change existed among the three types of plants: WT, BL-deficient *Sdet2* mutant, and WT grown on MS medium with 100 nM BL (WT + BL) (Fig. 4D). The use of scramble aptamer sequence in the AP did not lead to significant detection of BL in plant extracts (Fig. S13). The amount of BL in WT, *Sdet2*, and WT + BL was estimated to be ~89.7 pg, ~4.6 pg, and ~584.5 pg per gfw, respectively. In this assay, the detection limit of BL was estimated to be 0.6 pg $mL^{-1}$. It should be noted that exogenous treatment of BL with *Arabidopsis* WT can reduce the production of endogenous BL because BL signaling induces a negative feedback regulation that suppresses expression of BL biosynthetic genes (Kim and Wang, 2010). Therefore, compared to the BL detected in WT *Arabidopsis*, the redundant BL detected in BL-treated WT is likely to be exogenous, but not endogenous. Importantly, the significant difference in BL content between WT and the BL-deficient *Sdet2* mutant indicates that the AP-based assay is sufficiently capable of distinguishing endogenous BL levels due to its high sensitivity. In the plant kingdom, BL occurs at a considerably low concentration in vegetative tissues. In *Arabidopsis*, it was reported that picogram levels of BL per gfw were observed (Choe et al., 1999), consistent with the detection range of BL observed in this method. This result reveals that the AP-combined GNP colorimetric assay facilitates simple and sensitive BL detection in real plant samples owing to the pre-concentration effect of AP. It is not easy to measure BL using a traditional time-consuming method, such as gas chromatography-mass spectrometry.

The peroxidase-mimicking DNAzyme activity of the tgBPA-v2 aptamer with a BPA-induced G4 structure was examined in the presence of hemin (an iron-containing porphyrin derivative as a cofactor for DNAzyme), which can result in a strong blue color upon reactions with tetramethylbenzidine (TMB) and hydrogen peroxide ($H_2O_2$) (Fig. 5A) (Li et al., 2016; Travascio et al. 1998, 1999). Using this principle, a stronger TMB-oxidized color was observed when BPA was treated with the tgBPA-v2 aptamer than the other two selected aptamers (gBPA11-40 and tgBPA-v1) (Fig. 5B), confirming that tgBPA-v2 exhibited BPA concentration-dependency with high selectivity in solution (Fig. 5C) and indicating the enzymatic function of this aptamer as a BPA aptasensor. The detection limit of BPA was estimated to be 0.3 ng $mL^{-1}$. Moreover, based on the simple two-step (aptamer and reagent binding steps) and drop-on assay on thermal receipt papers (Fig. 5D), the tgBPA-v2 aptamer allowed for the rapid identification of BPA in thermal receipts (Fig. 5E). This target-induced enzymatic signal generation by the aptamer was observed for the first time in this study, contrary to the previously reported BPA aptamer, exhibiting a decrease in peroxidase activity upon binding with BPA (Fig. S14) (Jo et al., 2011; Xu et al., 2019). Collectively, these observations indicate that aptamers selected using GNP-SELEX are immediately suitable for sensing and assaying small molecules.

Despite recent advances in SELEX combined with nanomaterials or enrichment techniques, a visual monitoring process is required to reduce the time and cost associated with each SELEX round (Blind and Blank, 2015; Zhuo et al., 2017). In this study, we established a new role for GNPs as visual selectors in SELEX. In this regard, the developed GNP-SELEX has several advantages over classical SELEXs: (i) there is no need to modify small molecule targets, (ii) it enables real-time colorimetric progression with the naked eyes or simple extinction measurement, (iii) it allows for rapid determination of aptamer enrichment and round transition/termination without auxiliary analysis (e.g., real-time qPCR), which encompasses a real self-monitoring process, such as STOP (termination of positive or negative SELEX), BACK (to the round again), or GO (to the next round) in response to aptamer libraries in every round, and (iv) the process enables format extensibility and is extremely versatile for various positive and negative targets. As therapeutic and diagnostic aptamers have been proved in the market (Kaur et al., 2018; Kulabhusan et al., 2020), further progress on integrating this method with microfluidic or other low-cost automatic strategy (Dembowski and Bowser, 2017; Han et al., 2020) will facilitate the rapid discovery and practical use of aptamers.

## 4. Conclusions

We demonstrated GNP-SELEX as a simple and real-time monitoring SELEX platform to rapidly discover ssDNA aptamers against small molecules, such as BL or BPA. GNP-SELEX exhibited real-time monitoring within and between SELEX rounds and enabled the rapid and proofreading determination of aptamer library enrichment by leveraging the colorimetric change of GNPs in response to intact targets and aptamers. Through this process, small molecule-specific aptamers with high binding affinity were identified, and truncated aptamers (tgBL-v2 and tgBPA-v2) were designed using 3D molecular simulation, resulting in the development of aptasensors to effectively detect targets in real samples (plant extracts or thermal receipts). Owing to its simplicity and versatility, we suggest that GNP-SELEX will be useful as a colorimetric SELEX platform to facilitate the rapid discovery of ssDNA aptamers against various targets and identify their wide applications in bioassays and biosensors.

## CRediT authorship contribution statement

**Eun-Song Lee:** Investigation, Methodology, Validation, Writing – original draft. **Eun-Ji Kim:** Investigation, Resources. **Tae-Ki Park:** Investigation, Resources. **Da-Woon Bae:** Software, Investigation. **Sun-Shin Cha:** Software, Methodology, Investigation. **Tae-Wuk Kim:** Methodology, Supervision, Writing – review & editing. **Young-Pil Kim:** Conceptualization, Supervision, Methodology, Writing – review & editing.

## Declaration of competing interest

The authors declare that they have no known competing financial interests or personal relationships that could have appeared to influence the work reported in this paper.

## Acknowledgment

This work was supported by the National Research Foundation (NRF) grant funded by the Korean government (MSIT) (No.2016M3A9B4918833 to Y.-P.K.), the KIST Institutional Program (Project No. 2Z06270-20-137 to Y.-P.K.), and the Korea Environment Industry & Technology Institute (KEITI) through the Aquatic Ecosystem Conservation Research Program, funded by the Korea Ministry of Environment (MOE) (No. 2020003030007 to Y.-P.K.). This work was also supported by Basic Science Research Program (No. 2020R1A6A1A06046728) through the NRF funded by the Ministry of Education, Korea and supported by the Korea Polar Research Institute (KOPRI grant number PM21030 to S.-S.C.).

## Appendix A. Supplementary data

Supplementary data to this article can be found online at https://doi.org/10.1016/j.bios.2021.113468.

## References

Bailey, T.L., Boden, M., Buske, F.A., Frith, M., Grant, C.E., Clementi, L., Ren, J.Y., Li, W. W., Noble, W.S., 2009. Meme SUITE: tools for motif discovery and searching. Nucleic Acids Res. 37, W202–W208.

Blind, M., Blank, M., 2015. Aptamer selection Technology and recent advances. Mol. Ther. Nucleic Acids 4, e223.

Chang, A.L., McKeague, M., Liang, J.C., Smolke, C.D., 2014. Kinetic and equilibrium binding characterization of aptamers to small molecules using a label-free, sensitive, and scalable platform. Anal. Chem. 86 (7), 3273–3278.

Chatterjee, B., Kalyani, N., Anand, A., Khan, E., Das, S., Bansal, V., Kumar, A., Sharma, T. K., 2020. Gold SELEX: a novel SELEX approach for the development of high-affinity aptamers against small molecules without residual activity. Microchim Acta 187 (11), 618.

Cho, E.J., Lee, J.W., Ellington, A.D., 2009. Applications of aptamers as sensors. Annu. Rev. Anal. Chem. 2, 241–264.

Choe, S., Noguchi, T., Fujioka, S., Takatsuto, S., Tissier, C.P., Gregory, B.D., Ross, A.S., Tanaka, A., Yoshida, S., Tax, F.E., Feldmann, K.A., 1999. The *Arabidopsis* dwf7/ste 1 mutant is defective in the delta 7 sterol C-5 desaturation step leading to brassinosteroid biosynthesis. Plant Cell 11 (2), 207–221.

Dembowski, S.K., Bowser, M.T., 2017. Microfluidic methods for aptamer selection and characterization. Analyst 143 (1), 21–32.

Drolet, D.W., Moon-McDermott, L., Romig, T.S., 1996. An enzyme-linked oligonucleotide assay. Nat. Biotechnol. 14 (8), 1021–1025.

Gold, L., Polisky, B., Uhlenbeck, O., Yarus, M., 1995. Diversity of oligonucleotide functions. Annu. Rev. Biochem. 64, 763–797.

Gopinath, S.C., Lakshmipriya, T., Awazu, K., 2014. Colorimetric detection of controlled assembly and disassembly of aptamers on unmodified gold nanoparticles. Biosens. Bioelectron. 51, 115–123.

Grabar, K.C., Freeman, R.G., Hommer, M.B., Natan, M.J., 1995. Preparation and characterization of Au colloid monolayers. Anal. Chem. 67 (4), 735–743.

Han, Y.D., Chun, H.J., Yoon, H.C., 2020. Low-cost point-of-care biosensors using common electronic components as transducers. BioChip J 14 (1), 32–47.

Huang, C.C., Huang, Y.F., Cao, Z., Tan, W., Chang, H.T., 2005. Aptamer-modified gold nanoparticles for colorimetric determination of platelet-derived growth factors and their receptors. Anal. Chem. 77 (17), 5735–5741.

Jo, M., Ahn, J.Y., Lee, J., Lee, S., Hong, S.W., Yoo, J.W., Kang, J., Dua, P., Lee, D.K., Hong, S., Kim, S., 2011. Development of single-stranded DNA aptamers for specific bisphenol A detection. Oligonucleotides 21 (2), 85–91.

Kanwar, M.K., Bajguz, A., Zhou, J., Bhardwaj, R., 2017. Analysis of brassinosteroids in plants. J. Plant Growth Regul. 36 (4), 1002–1030.

Kaur, H., Bruno, J.G., Kumar, A., Sharma, T.K., 2018. Aptamers in the therapeutics and diagnostics pipelines. Theranostics 8 (15), 4016–4032.

Kim, T.W., Wang, Z.Y., 2010. Brassinosteroid signal transduction from receptor kinases to transcription factors. Annu. Rev. Plant Biol. 61, 681–704.

Kulabhusan, P.K., Hussain, B., Yuce, M., 2020. Current perspectives on aptamers as diagnostic tools and therapeutic agents. Pharmaceutics 12 (7), 646.

Lee, E.-S., Kim, G.B., Ryu, S.-H., Kim, H., Yoo, H.H., Yoon, M.Y., Lee, J.-W., Gye, M.C., Kim, Y.-P., 2018. Fluorescing aptamer-gold nanosensors for enhanced sensitivity to bisphenol A. Sensor. Actuator. B Chem. 260, 371–379.

Li, L., Li, B., Qi, Y., Jin, Y., 2009. Label-free aptamer-based colorimetric detection of mercury ions in aqueous media using unmodified gold nanoparticles as colorimetric probe. Anal. Bioanal. Chem. 393 (8), 2051–2057.

Li, W., Li, Y., Liu, Z., Lin, B., Yi, H., Xu, F., Nie, Z., Yao, S., 2016. Insight into G-quadruplex-hemin DNAzyme/RNAzyme: adjacent adenine as the intramolecular species for remarkable enhancement of enzymatic activity. Nucleic Acids Res. 44 (15), 7373–7384.

Li, W., Luo, Y., Gao, T., Yang, L., Wang, J., Pei, R., 2019. In vitro selection of DNA aptamers for a small-molecule porphyrin by gold nanoparticle-based SELEX. J. Mol. Evol. 87 (7–8), 231–239.

Liu, J., Lu, Y., 2005. Fast colorimetric sensing of adenosine and cocaine based on a general sensor design involving aptamers and nanoparticles. Angew. Chem. Int. Ed. 45 (1), 90–94.

Luo, Z., He, L., Wang, J., Fang, X., Zhang, L., 2017. Developing a combined strategy for monitoring the progress of aptamer selection. Analyst 142 (17), 3136–3139.

Ma, H., Liu, J., Ali, M.M., Mahmood, M.A., Labanieh, L., Lu, M., Iqbal, S.M., Zhang, Q., Zhao, W., Wan, Y., 2015. Nucleic acid aptamers in cancer research, diagnosis and therapy. Chem. Soc. Rev. 44 (5), 1240–1256.

Mendonsa, S.D., Bowser, M.T., 2004. In vitro evolution of functional DNA using capillary electrophoresis. J. Am. Chem. Soc. 126 (1), 20–21.

Muller, J., El-Maarri, O., Oldenburg, J., Potzsch, B., Mayer, G., 2008. Monitoring the progression of the in vitro selection of nucleic acid aptamers by denaturing high-performance liquid chromatography. Anal. Bioanal. Chem. 390 (4), 1033–1037.

Nguyen, V.T., Kwon, Y.S., Kim, J.H., Gu, M.B., 2014. Multiple GO-SELEX for efficient screening of flexible aptamers. Chem. Commun. 50 (72), 10513–10516.

Noguchi, T., Fujioka, S., Choe, S., Takatsuto, S., Tax, F.E., Yoshida, S., Feldmann, K.A., 2000. Biosynthetic pathways of brassinolide in *Arabidopsis*. Plant Physiol 124 (1), 201–209.

Park, C.H., Jang, M.-S., Yun, J.H., Lee, J.E., Kim, M.K., Park, S.-C., Kim, S.-K., 2014. Effects of secondary mutation in det 2-1 on root growth and development in *Arabidopsis*. J. Plant Biol. 57 (4), 255–263.

Pfeiffer, F., Tolle, F., Rosenthal, M., Brandle, G.M., Ewers, J., Mayer, G., 2018. Identification and characterization of nucleobase-modified aptamers by click-SELEX. Nat. Protoc. 13 (5), 1153–1180.

Ruscito, A., DeRosa, M.C., 2016. Small-molecule binding aptamers: selection strategies, characterization, and applications. Front. Chem. 4, 14.

Smith, M., 2014. Gold Nanoparticles as a Platform for Small Molecule SELEX. Master's Thesis. Carleton University.

Smith, J.E., Chávez, J.L., Hagen, J.A., Kelley-Loughnane, N., 2016. Design and development of aptamer–gold nanoparticle based colorimetric assays for in-the-field applications. JoVE-J. Vis. Exp. 112, e54063.

Strehlitz, B., Nikolaus, N., Stoltenburg, R., 2008. Protein detection with aptamer biosensors. Sensors 8 (7), 4296–4307.

Thompson, M.J., Mandava, N.B., Meudt, W.J., Lusby, W.R., Spaulding, D.W., 1981. Synthesis and biological activity of brassinolide and its 22 beta, 23 beta-isomer: novel plant growth-promoting steroids. Steroids 38 (5), 567–580.

Tolle, F., Wilke, J., Wengel, J., Mayer, G., 2014. By-product formation in repetitive PCR amplification of DNA libraries during SELEX. PloS One 9 (12), e114693.

Travascio, P., Bennet, A.J., Wang, D.Y., Sen, D., 1999. A ribozyme and a catalytic DNA with peroxidase activity: active sites versus cofactor-binding sites. Chem. Biol. 6 (11), 779–787.

Travascio, P., Li, Y., Sen, D., 1998. DNA-enhanced peroxidase activity of a DNA-aptamer-hemin complex. Chem. Biol. 5 (9), 505–517.

Turkevich, J., Stevenson, P.C., Hillier, J., 1951. A study of the nucleation and growth processes in the synthesis of colloidal gold. J. Faraday Soc. 11, 55–75.

Wang, T., Chen, C., Larcher, L.M., Barrero, R.A., Veedu, R.N., 2019. Three decades of nucleic acid aptamer technologies: lessons learned, progress and opportunities on aptamer development. Biotechnol. Adv. 37 (1), 28–50.

Wei, H., Li, B., Li, J., Wang, E., Dong, S., 2007. Simple and sensitive aptamer-based colorimetric sensing of protein using unmodified gold nanoparticle probes. Chem. Commun. 36, 3735–3737.

Xu, J., Lee, E.S., Gye, M.C., Kim, Y.P., 2019. Rapid and sensitive determination of bisphenol A using aptamer and split DNAzyme. Chemosphere 228, 110–116.

Yang, W., Yu, H., Alkhamis, O., Liu, Y., Canoura, J., Fu, F., Xiao, Y., 2019. In vitro isolation of class-specific oligonucleotide-based small-molecule receptors. Nucleic Acids Res. 47 (12), e71.

Zhu, Z., Ravelet, C., Perrier, S., Guieu, V., Fiore, E., Peyrin, E., 2012. Single-stranded DNA binding protein-assisted fluorescence polarization aptamer assay for detection of small molecules. Anal. Chem. 84 (16), 7203–7211.

Zhu, Z., Yang, C., Zhou, X., Qin, J., 2011. Label-free aptamer-based sensors for L-argininamide by using nucleic acid minor groove binding dyes. Chem. Commun. 47 (11), 3192–3194.

Zhuo, Z., Yu, Y., Wang, M., Li, J., Zhang, Z., Liu, J., Wu, X., Lu, A., Zhang, G., Zhang, B., 2017. Recent advances in SELEX Technology and aptamer applications in biomedicine. Int. J. Mol. Sci. 18 (10).

Zuker, M., 2003. Mfold web server for nucleic acid folding and hybridization prediction. Nucleic Acids Res. 31 (13), 3406–3415.